Transcriptomic analysis of CFTR-impaired endothelial cells reveals a pro-inflammatory phenotype

Mathias Declercq[1,2,3], Pauline de Zeeuw[2,3], Nadine V. Conchinha[2,3], Vincent Geldhof[2,3], Anabela S. Ramalho[4], Melissa García-Caballero[2,3], Katleen Brepoels[2,3], Marjolein Ensinck[5], Marianne S. Carlon[5], Matthew J. Bird[6,7], Stefan Vinckier[2,3], Marijke Proesmans[8], François Vermeulen[9], Lieven Dupont[10], Bart Ghesquière[7,11], Mieke Dewerchin[2,3], Peter Carmeliet[2,3], David Cassiman[6,12], Lucas Treps[2,3,13], Guy Eelen[2,3,13] and Peter Witters[1,8,12,13]

@ERSpublications
CFTR-impaired endothelial cells have a pro-inflammatory phenotype that can attract and reinforce leukocyte extravasation. Endothelial cells possibly contribute to the excessive inflammatory phenotype observed in cystic fibrosis. https://bit.ly/2GRijq8

Cite this article as: Declercq M, de Zeeuw P, Conchinha NV, *et al.* Transcriptomic analysis of CFTR-impaired endothelial cells reveals a pro-inflammatory phenotype. *Eur Respir J* 2021; 57: 2000261 [https://doi.org/10.1183/13993003.00261-2020].

ABSTRACT Cystic fibrosis (CF) is a life-threatening disorder characterised by decreased pulmonary mucociliary and pathogen clearance, and an exaggerated inflammatory response leading to progressive lung damage. CF is caused by bi-allelic pathogenic variants of the cystic fibrosis transmembrane conductance regulator (CFTR) gene, which encodes a chloride channel. CFTR is expressed in endothelial cells (ECs) and EC dysfunction has been reported in CF patients, but a role for this ion channel in ECs regarding CF disease progression is poorly described.

We used an unbiased RNA sequencing approach in complementary models of CFTR silencing and blockade (by the CFTR inhibitor CFTRinh-172) in human ECs to characterise the changes upon CFTR impairment. Key findings were further validated *in vitro* and *in vivo* in CFTR-knockout mice and *ex vivo* in CF patient-derived ECs.

Both models of CFTR impairment revealed that EC proliferation, migration and autophagy were downregulated. Remarkably though, defective CFTR function led to EC activation and a persisting pro-inflammatory state of the endothelium with increased leukocyte adhesion. Further validation in CFTR-knockout mice revealed enhanced leukocyte extravasation in lung and liver parenchyma associated with increased levels of EC activation markers. In addition, CF patient-derived ECs displayed increased EC activation markers and leukocyte adhesion, which was partially rescued by the CFTR modulators VX-770 and VX-809.

Our integrated analysis thus suggests that ECs are no innocent bystanders in CF pathology, but rather may contribute to the exaggerated inflammatory phenotype, raising the question of whether normalisation of vascular inflammation might be a novel therapeutic strategy to ameliorate the disease severity of CF.

This article has supplementary material available from erj.ersjournals.com

Received: 7 Feb 2020 | Accepted: 4 Oct 2020

Introduction

Cystic fibrosis (CF) is an autosomal recessive disorder caused by impaired function of the cystic fibrosis transmembrane conductance regulator (CFTR) protein, which primarily acts as a chloride channel, mainly in epithelial cells [1]. CF is a multi-systemic disorder characterised by progressive lung disease and pancreatic insufficiency, while also featuring conditions of gastrointestinal involvement, liver disease and diabetes [2]. Lung disease determines much of the morbidity and mortality in CF patients [3]. While the CF lung phenotype is considered to be primarily caused by infections [3], the subsequent inflammation is simultaneously exaggerated and ineffective at eradicating pathogens, initiating a vicious cycle of infection and inflammation [4]. Persistent high-intensity inflammation inflicts permanent structural damage on the airways and impairs lung function, which ultimately results in respiratory failure and death [3, 4].

Endothelial cells (ECs) line the inner wall of blood vessels [5]. These cells regulate blood clotting, inflammation, angiogenesis and vascular tone [6]. Although CFTR is expressed and functional in normal ECs [7, 8], the vascular role of CFTR is less well studied in comparison to its well-established role in epithelial cells. Yet, micro- and macrovascular dysfunction have been documented in CF patients [9, 10]. Endothelial dysfunction is involved in CF-associated manifestations including diabetes and cardiovascular-, lung- and liver-associated complications [11, 12]. Nevertheless, the underlying mechanism of EC dysfunction and its role in disease progression remain elusive [11, 12]. Endothelial dysfunction is a predictor of cardiovascular risk, and genome-wide association studies detected a link between single-nucleotide polymorphisms in *CFTR* and coronary artery disease and flow-mediated arterial dilation [13, 14]. Elucidating the role of CFTR in ECs is therefore relevant for understanding the pathophysiology of CF and cardiovascular diseases [13, 14]. We thus employed an unbiased transcriptomics approach complemented by functional characterisation of EC properties upon CFTR impairment, and studied the possible relevance of our findings for CF patients.

Materials and methods

Details regarding materials and methods are provided in the supplementary material.

Cell culture

Freshly isolated human umbilical vein endothelial cells (HUVECs) were obtained from different donors and used as single-donor cultures between passage 1 and 4 as previously described [15, 16]. Blood outgrowth endothelial cells (BOECs) were freshly isolated from peripheral blood obtained from different healthy donors and CF patients from the outpatient clinic in their usual state of health without intercurrent infections (clinical information is shown in supplementary table S1) following previously described protocols with minor modifications [17, 18].

In vivo *mouse assays*

Leukocyte infiltration into lung and liver was analysed as previously described with minor adaptations [19]. Briefly, Cftr^{tm1Unc}-Tg(FABPCFTR)1Jaw/J (CFTR knockout (CFTR^{KO})) mice [20, 21] were perfused with PBS and organs were collected for immunostaining (CD45 and CD105) or digested for flow cytometry analysis (CD45, CD31, intercellular adhesion molecule 1 (ICAM1) and vascular cell adhesion molecule 1 (VCAM1)).

Bulk RNA sequencing and analysis

RNA extracted with TRIzol was subjected to sequencing library preparation with the Lexogen QuantSeq 3′ mRNA-Seq library preparation kit (Lexogen, Vienna, Austria). Samples were indexed to allow for multiplexing. Library quality and size range was assessed using a Bioanalyzer (Agilent Technologies,

Affiliations: [1]Dept of Development and Regeneration, CF Centre, Woman and Child, KU Leuven, Leuven, Belgium. [2]Laboratory of Angiogenesis and Vascular Metabolism, Centre for Cancer Biology, VIB, Leuven, Belgium. [3]Laboratory of Angiogenesis and Vascular Metabolism, Dept of Oncology and Leuven Cancer Institute (LKI), KU Leuven, Leuven, Belgium. [4]Stem Cell and Developmental Biology, CF Centre, Woman and Child, KU Leuven, Leuven, Belgium. [5]Laboratory for Molecular Virology and Drug Discovery, Dept of Pharmaceutical and Pharmacological Sciences, KU Leuven, Leuven, Belgium. [6]Laboratory of Hepatology, Dept of Chronic Diseases, Metabolism and Ageing, KU Leuven, Leuven, Belgium. [7]Metabolomics Expertise Centre, Centre for Cancer Biology, VIB, Leuven, Belgium. [8]Dept of Paediatrics, University Hospitals Leuven, Leuven, Belgium. [9]Dept of Respiratory Diseases, University Hospitals Leuven, Leuven, Belgium. [10]Dept of Pneumology, University Hospitals Leuven, Leuven, Belgium. [11]Metabolomics Expertise Centre, Dept of Oncology, KU Leuven, Leuven, Belgium. [12]Centre of Metabolic Diseases, University Hospitals Leuven, Leuven, Belgium. [13]Equal co-authorship.

Correspondence: Peter Witters, University Hospitals Leuven, Dept of Paediatrics and Centre of Metabolic Diseases, Herestraat 49, Box 7003 20, 3000 Leuven, Belgium. E-mail: peter.witters@uzleuven.be

Leuven, Belgium) with the DNA 1000 kit (Agilent Technologies). Libraries (2 nM) were sequenced on an Illumina HiSeq 4000 platform (Illumina, Eindhoven, the Netherlands). Single-end reads of 50 bp length were produced with a minimum of 1 M reads per sample. Quality control of raw reads was performed with FastQC v0.11.7 [22].

Immunoblotting

Protein extraction and immunoblot analysis were performed using a modified Laemmli sample buffer (125 mM Tris-HCl, pH 6.8 buffer containing 2% SDS and 10% glycerol) in the presence of protease and phosphatase inhibitors (Roche, Anderlecht, Belgium). Mitochondrial isolation was performed using the mitochondria isolation kit for cultured cells according to the manufacturer's instructions (Thermo Fisher Scientific, Geel, Belgium). Lysates were separated by SDS-PAGE under reducing conditions, transferred to a nitrocellulose membrane, and analysed by immunoblotting.

In vitro *functional assays*

Endothelial proliferation, lactate dehydrogenase (LDH) viability assay, scratch wound, trans-endothelial electrical resistance (TEER) and leukocyte adhesion assays were performed as described previously [19, 23–25].

Intracellular and mitochondrial reactive oxygen species analysis

Intracellular and mitochondrial reactive oxygen species (ROS) levels were measured using CM-H_2DCFDA (Thermo Fisher Scientific) and MitoSOX (Thermo Fisher Scientific) according to the manufacturer's instructions, and quantified as previously described [26].

Oxygen consumption rate

Bioenergetics of ECs were determined on a Seahorse XF24 instrument (Agilent, Diegem, Belgium) as previously described [27].

Detection of glutathione species and NADPH

Targeted metabolites were measured as previously described [27].

Quantification and statistical analysis

Data represent mean±SEM of at least three independent experiments. Statistical significance was calculated by standard two-tailed t-test (with Welch's correction when variances were significantly different between groups), ANOVA (for multiple comparisons within one dataset) and one-sample t-test (for comparisons to point normalised data) using Prism v8.2 (GraphPad Software, La Jolla, CA, USA). Bioinformatic analysis was carried out using in-house-developed BIOMEX software [28]. A p-value <0.05 was considered statistically significant.

Results

CFTR impairment leads to transcriptomic alterations in ECs

We first confirmed earlier findings [7, 8] of detectable CFTR expression in cultured primary HUVECs (hereafter referred to as ECs) at the protein level *via* immunoblotting and immunocytochemistry (figure 1a, b). In many cases, CFTR mutations result in lower levels of functional CFTR protein in the plasma membrane [29]. To study CFTR's function, we therefore used two complementary models to mimic this situation: 1) we blocked CFTR activity using the allosteric CFTR inhibitor CFTRinh-172, which is commonly used in CF research [30]; and 2) we silenced CFTR expression using lentiviral-mediated expression of two non-overlapping CFTR-specific short hairpin RNAs (shRNAs) to obtain a CFTR knockdown ($CFTR^{KD}$). We refer to CFTR-blocked or CFTR-silenced ECs as "CFTR-impaired" ECs.

$CFTR^{KD}$ lowered CFTR protein levels by >55% (figure 1a–c, supplementary figure S1a) without altering protein expression of the typical endothelial markers von Willebrand factor and vascular endothelial cadherin (VE-cadherin) (supplementary figure S1b). While CFTR blockade or silencing only minimally affected EC survival (supplementary figure S1c, d), increasing $CFTR^{KD}$ efficiency (>95% at the protein level) increased cell death (>50%, supplementary figure S1d, e). We therefore performed further experiments at an intermediate silencing depth.

We carried out an unbiased transcriptomics analysis to screen for global changes induced upon CFTR impairment. Principal component analysis of all genes and hierarchical clustering analysis of the highly variable genes revealed that control and CFTR-impaired ECs grouped into distinct clusters, suggesting broad transcriptomic changes (figure 1d, e, supplementary figure S2a, b). Gene set enrichment analysis (GSEA) comparing control and CFTR-impaired ECs was used to associate groups of significantly differentially expressed genes with biological processes (supplementary table S2) [31]. Upon CFTR impairment, GSEA revealed increased expression of pro-inflammatory, ion transmembrane transport and

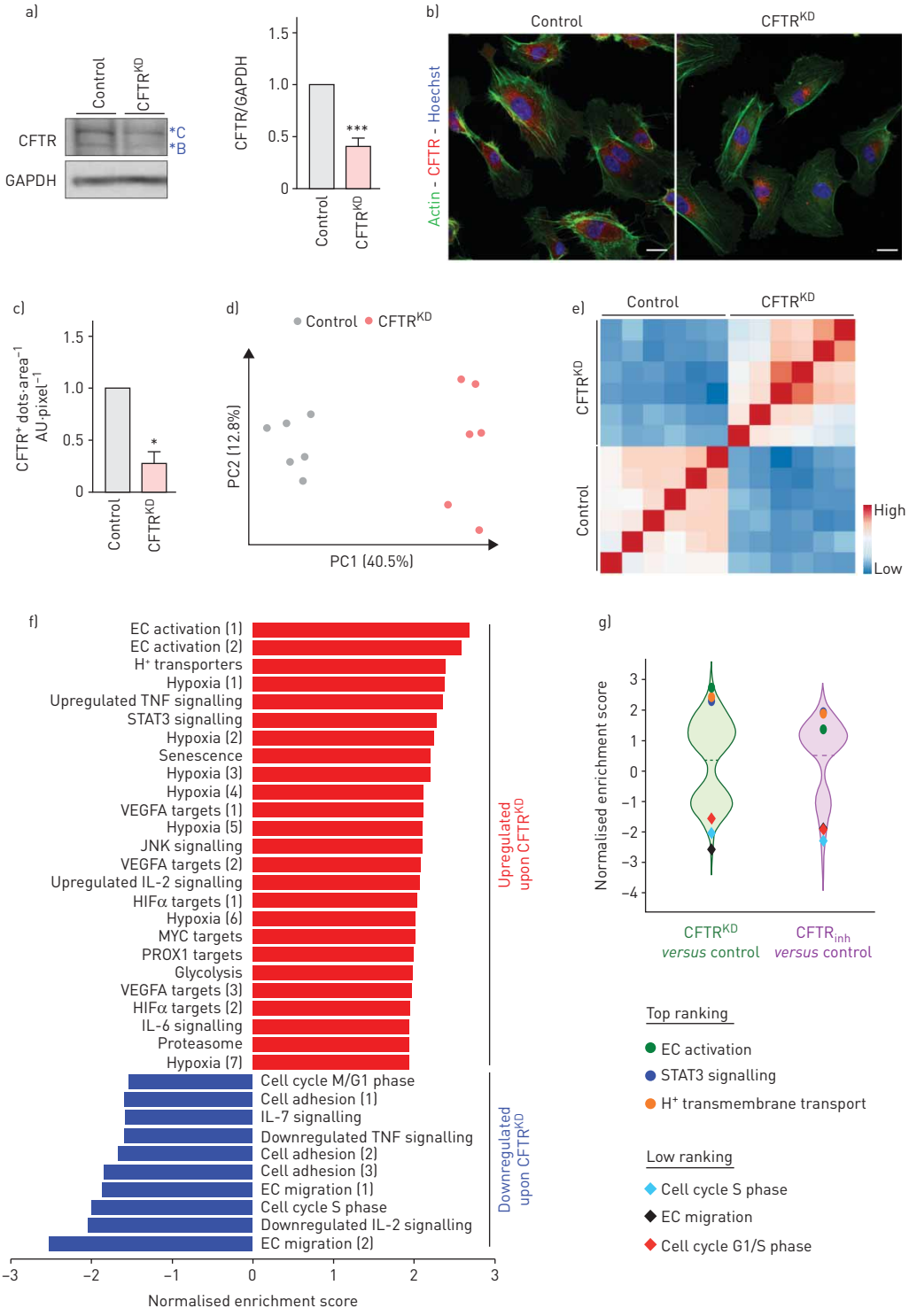

FIGURE 1 Transcriptomic signature of cystic fibrosis transmembrane conductance regulator (CFTR)-silenced endothelial cells (ECs). a) Representative immunoblot for CFTR expression in ECs transduced with scrambled short hairpin RNA (shRNA) (control) or CFTR shRNA (CFTR^{KD}). Bands B and C indicate immature (native) and mature (glycosylated) CFTR respectively. GAPDH was used as loading control. Densitometric quantification of the ratio of CFTR to GAPDH is shown on the right. Data are presented as mean+SEM; n=10. ***: p<0.001 by one-sample t-test. b) Representative confocal images of control and CFTR^{KD} ECs stained for CFTR (red), actin (green) and nuclei (Hoechst; blue). Scale bar: 100 µm. c) Fluorescence quantification of control and CFTR^{KD} ECs. Data are presented as mean+SEM; n=3. *: p<0.05 by one-sample t-test. AU: arbitrary units. d) Principal component (PC) analysis on all genes of control and CFTR^{KD} ECs obtained after bulk RNA sequencing. e) Correlation heatmap of the highly variable genes in control and CFTR^{KD} ECs. Colour scale: red, high correlation; blue, low correlation. f) Bar plots representing the top deregulated gene sets (with a significant adjusted p-value) ranked based on their normalised enrichment score. For official gene set names see supplementary table S2. Numbers between parentheses indicate alternative gene sets pertaining to the same biological function or signalling pathway. g) Violin plots representing top-ranking (dots) and low-ranking (diamonds) gene sets obtained after meta-analysis of control *versus* CFTR-impaired ECs (CFTR^{KD} and CFTRinh-172- treated (CFTR$_{inh}$)). Symbols indicate where gene sets are located in the distribution.

hypoxia-related pathways, while gene sets involved in proliferation (cell cycle), cell migration and cell adhesion were downregulated (figure 1f, supplementary figure S2c, supplementary table S2).

We then set out to obtain congruent markers that are conserved across CFTR blockade and silencing. We hypothesised that congruent pathways are related to the chloride channel function of CFTR, whose malfunction is shared between all CF patients. Congruent upregulated gene sets suggested a role in EC activation (pathways related to tumour necrosis factor-α (TNF-α), signal transducer and activator of transcription 3 (STAT3), hypoxia-inducible factor 1-α (HIF1-α), interleukin (IL)-2 and IL-6), antigen binding and processing (human leukocyte antigen (HLA) class I, transporters associated with antigen processing and cathepsins), matrisome remodelling and ion transmembrane transport, while congruent downregulated gene sets implied a possible role in the cell cycle, migration and adhesion (supplementary figure S2d, supplementary table S3). We confirmed these findings by performing a meta-analysis of control *versus* CFTR-impaired ECs to rank differentially regulated genes and gene sets (figure 1g, supplementary table S3). Among the top 20 ranking genes were *CD9*, *CYR61*, *CXCL1* and *CCL2*, which have been linked to leukocyte recruitment to the endothelial membrane and trans-endothelial leukocyte migration (supplementary table S3) [32–35]. The top three upregulated gene sets were involved in EC activation, STAT3 signalling and H^+ transmembrane transport, while gene sets involved in the cell cycle and cell migration were the top three downregulated gene sets (figure 1g, supplementary table S3). Taken together, CFTR impairment induced a prominent pro-inflammatory and EC activation gene signature, accompanied by a downregulated gene signature of EC migration and proliferation.

Several key EC functions malfunction upon CFTR impairment

To investigate in more detail the compromised EC proliferation transcriptome signature upon CFTR silencing, we compared the expression of genes involved in various phases of the cell cycle. Genes coding for proliferation markers, transcriptional regulators, cyclins and cyclin-dependent kinases were downregulated upon CFTR impairment (figure 2a). These transcriptomic findings were confirmed by a decrease in EC proliferation as measured by tritium-labelled thymidine incorporation into DNA upon CFTR impairment (figure 2b, c).

The transcriptomics analysis further revealed that CFTR silencing downregulated the expression of genes involved in integrin and vascular endothelial growth factor (VEGF) signalling, and actin remodelling, suggesting a novel role of CFTR in EC migration (figure 2d). In agreement, the scratch wound assay confirmed reduced migration of CFTR-impaired ECs (figure 2e, f). Overexpression of an exogenous haemaglutinine (HA)-tagged CFTR in ECs (to facilitate visualisation) followed by immunostaining for the HA-tag revealed that CFTR was primarily expressed and enriched in membrane ruffling structures (*e.g.* lamellipodia) of migrating ECs (supplementary figure S3a), further supporting a role in EC migration. Confluent monolayers of $CFTR^{KD}$ ECs displayed compromised junctional integrity as measured by a higher proportion of discontinuous and reticulated VE-cadherin and CD31 junctions (figure 2g, h, supplementary figure S3b, c) [18, 36, 37]. Functionally, this corresponded to a decrease in the trans-endothelial electrical resistance (TEER) of CFTR-impaired ECs (figure 2i, j), which is in line with previously published findings on ECs in CF [38, 39]. Our data thus indicate an underappreciated role for CFTR in EC proliferation and migration, and in maintaining endothelial barrier integrity.

CFTR impairment induces oxidative stress and mitochondrial dysfunction

Increased oxidative stress is a well-known and noxious hallmark of CF pathophysiology [40]. CFTR silencing led to the induction of several gene classes related to an anti-oxidative stress response, including transcription factors capable of binding antioxidant response elements (ARE), glutathione-consuming enzymes, superoxide dismutase, peroxiredoxin, thioredoxin, and DNA repair and chaperone proteins (figure 3a). We confirmed these transcriptomic changes by flow cytometry analysis of total cellular oxidative stress, which indeed revealed increased oxidative stress upon CFTR impairment (figure 3b, c). When key cellular antioxidant scavengers were measured by liquid chromatography-mass spectrometry, both glutathione (GSH) and its reducing co-factor NADPH were affected, as indicated by the increased ratios of oxidised/total GSH and $NADP^+$/NADPH (figure 3d–g). The mRNA transcript levels of glutamate-cysteine ligase, the rate-controlling enzyme in GSH biosynthesis, were unchanged in CFTR-silenced ECs (supplementary figure S4a), suggesting that increased GSH consumption rather than reduced GSH synthesis contributed to the elevated oxidative stress.

Measurements of mitochondrial ROS using the MitoSOX dye by flow cytometry revealed that CFTR impairment led to significantly elevated mitochondrial O^{2-} levels (figure 3h, i). This was associated with decreased mitochondrial respiration as reflected by a reduced basal oxygen consumption rate, ATP production and maximal oxygen consumption rate (figure 3j–m), suggesting mitochondriopathy.

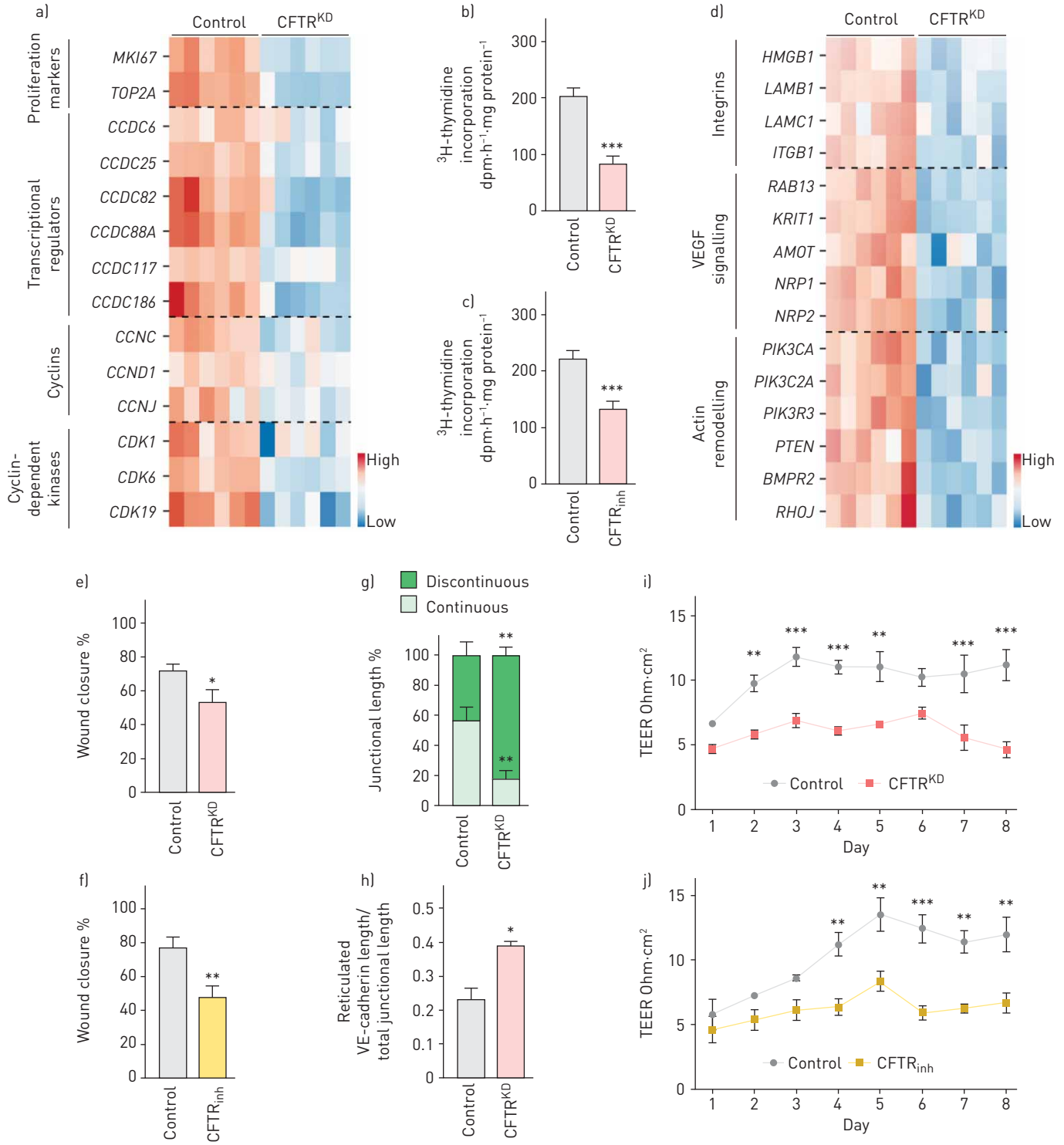

FIGURE 2 Endothelial proliferation and migration are reduced upon cystic fibrosis transmembrane conductance regulator (CFTR) impairment. a) Heatmap showing the expression levels of differentially expressed genes between endothelial cells (ECs) transduced with scrambled short hairpin RNA (shRNA) (control) or CFTR shRNA ($CFTR^{KD}$). Selected genes are involved in cell proliferation and have adjusted p-values<0.05. Colour scale: red, high feature expression; blue, low feature expression. b, c) [^{3}H]-thymidine incorporation into DNA (proliferation assay) in control versus $CFTR^{KD}$ ECs (n=10) (b) or DMSO-treated control ECs *versus* CFTRinh-172-treated ECs ($CFTR_{(inh)}$) (n=6) (c). Data are presented as mean+SEM. ***: p<0.001 by two-tailed paired t-test. d) Heatmap showing differentially expressed genes important in cell migration between control and $CFTR^{KD}$ ECs. Selected genes have adjusted p-values<0.05. e, f) Scratch wound migration assay with control and CFTR-impaired ECs ($CFTR^{KD}$, n=8 (e) or $CFTR_{inh}$, n=7 (f)). Data are presented as mean+SEM. *: p<0.05; **: p<0.01 by two-tailed paired t-test. g, h) Quantification of the fraction of discontinuous and continuous VE-cadherin-stained junctions (n=4) (g) and the fraction of reticulated VE-cadherin junctions in control and $CFTR^{KD}$ ECs (n=5) (h). Data are presented as mean+SEM. *: p<0.05; **: p<0.01 by two-tailed unpaired t-test. i, j) Trans-endothelial electrical resistance (TEER) assay with control and CFTR-impaired ECs ($CFTR^{KD}$, n=3 (i) or $CFTR_{inh}$, n=3 (j)). Data are presented as mean±SEM. **: p<0.01; ***: p<0.001 by two-way ANOVA.

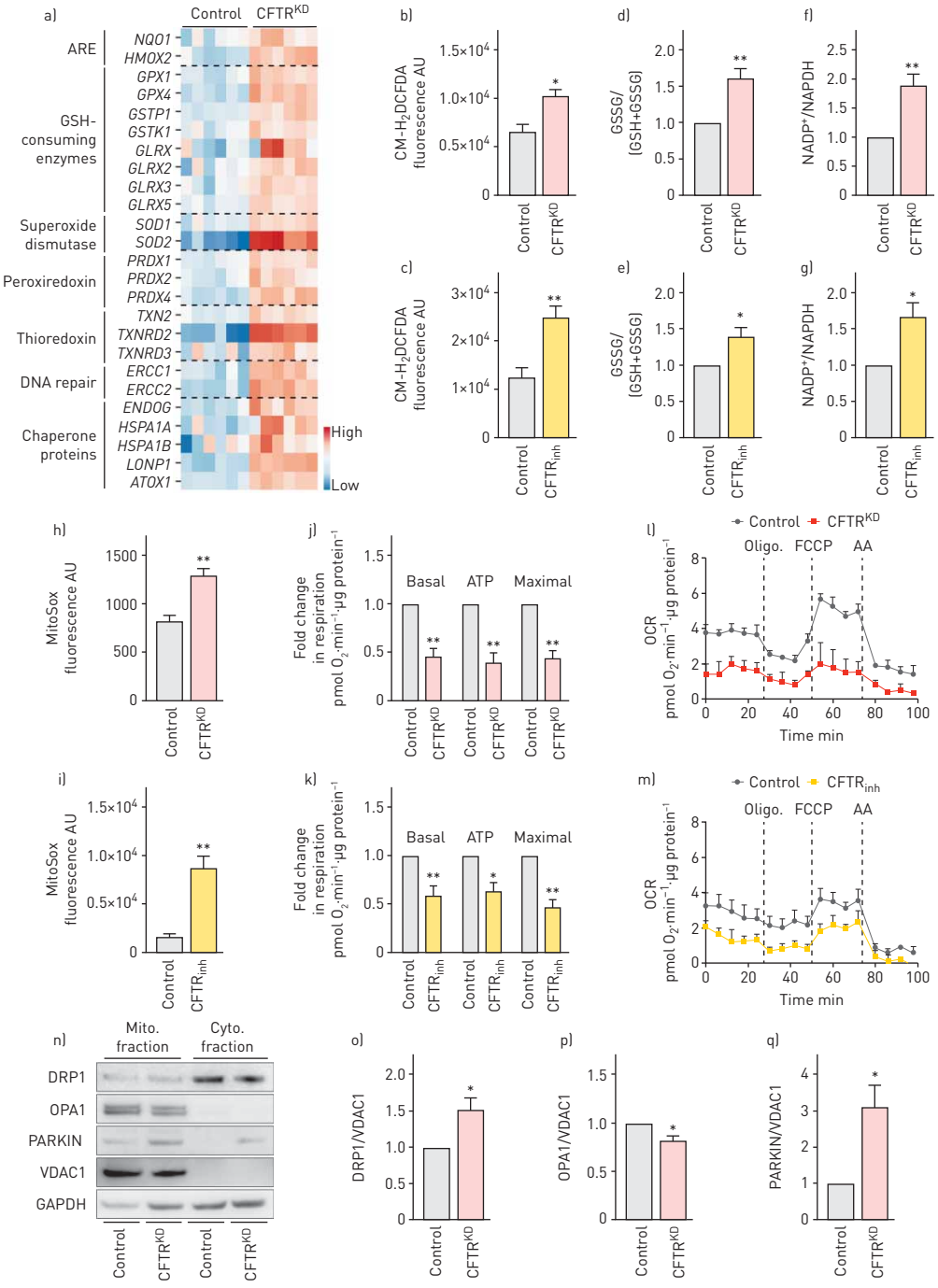

FIGURE 3 Cystic fibrosis transmembrane conductance regulator (CFTR) defect in endothelial cells (ECs) induces oxidative stress and mitochondrial dysfunction. a) Heatmap showing the expression levels of differentially expressed genes between ECs transduced with scrambled short hairpin RNA (shRNA) (control) or CFTR shRNA ($CFTR^{KD}$). Selected genes are involved in cell response to oxidative stress and have adjusted p-values<0.05. Colour scale: red, high feature expression; blue, low feature expression. ARE: transcription factors binding antioxidant response elements. b–g) Intracellular reactive oxygen species (ROS) levels (CM-H_2DCFDA) measured by flow cytometry and expressed in arbitrary units (AU) in control *versus* $CFTR^{KD}$ ECs (b) or DMSO-treated control ECs *versus* CFTRinh-172-treated ECs ($CFTR_{inh}$) (c). (GSSG)/(GSH+GSSG) ratio in control *versus* $CFTR^{KD}$ ECs (d) or DMSO-treated control ECs *versus* $CFTR_{inh}$ ECs (e). $NADP^+$/NADPH ratios measured by liquid chromatography-mass spectrometry and normalised to protein content in control *versus* $CFTR^{KD}$ ECs (f) or DMSO-treated control ECs *versus* $CFTR_{inh}$ ECs (g). Data are presented as mean+SEM; $CFTR^{KD}$ n=4; $CFTR_{inh}$ n=4. *: p<0.05; **: p<0.01 by one-sample t-test. h, i) Mitochondrial ROS levels, measured by flow cytometry after incubation with the MitoSOX dye. Data are presented as mean+SEM; $CFTR^{KD}$ n=3; $CFTR_{inh}$ n=6. **: p<0.01 by two-tailed paired t-test. j–m) Basal, ATP-producing and maximal oxygen consumption rates (OCRs) were measured by Seahorse after oligomycin (Oligo.), carbonyl cyanide-p-trifluoromethoxy phenylhydrazone (FCCP) and antimycin A (AA) treatments. Data are presented as mean+SEM; $CFTR^{KD}$ n=4; $CFTR_{inh}$ n=4. *: p<0.05; **: p<0.01 by one-sample t-test. n) Representative immunoblots for dynamin related protein 1 (DRP1) (mitochondrial fission), OPA1 mitochondrial dynamin like GTPase (OPA1) (mitochondrial fusion) and Parkin (mitophagy) in control or $CFTR^{KD}$ ECs and subjected to mitochondrial (mito.) and cytoplasmic (cyto.) fractionation. VDAC1 was used as loading control for mitochondrial fraction, while GAPDH was used for the cytoplasmic fraction. o–q) Densitometric quantifications. Data are presented as mean+SEM; n=5. *: p<0.05 by one-sample t-test.

The clearance of damaged mitochondria through autophagy, a process called mitophagy, is vital for cellular functioning and survival [41]. Immunoblotting revealed increased mitochondrial levels of dynamin related protein 1 (DRP1) and Parkin (mediating mitochondrial fission), but reduced levels of OPA1 mitochondrial dynamin like GTPase (OPA1) (mediating mitochondrial fusion), indicative of increased mitochondrial fission but reduced fusion (figure 3n–q). Taken together, these data show that CFTR deficiency induces an oxidative stress response, with more damaged mitochondria with defective mitochondrial function.

Autophagy deficiency in CFTR-impaired ECs

Differential gene expression analysis of our transcriptomic data revealed that autophagy markers p62 (*SQSTM1*) and microtubule-associated protein 1 light chain 3B (LC3B) (*MAP1LC3B*) were elevated upon CFTR silencing (figure 4a). Real-time qPCR analysis of these marker genes confirmed these findings (figure 4b). Corroboratively, the protein levels of the autophagic substrate p62 and autophagosome markers LC3BI and LC3BII were also increased (figure 4c–j), suggesting an accumulation of autophagosomes and a defect in autophagy flux rather than increased functional autophagy. To validate our findings, we performed transmission electron microscopy (TEM), which highlighted a two-fold increase in autophagosome abundance upon CFTR impairment, confirming defective autophagy (figure 4k–n, supplementary figure S4b). $CFTR^{KD}$ ECs displayed upregulated mTORC1 activity (a known inhibitor of autophagosome formation and lysosome biogenesis [42]) as measured by the increased phosphorylation of its downstream canonical target P70S6K and its substrate S6 (figure 4o–r). Our results suggest that CFTR impairment may hinder endothelial autophagy through mTORC1 activation and autophagosome accumulation.

CFTR impairment induces EC activation

Differential expression analysis in control *versus* $CFTR^{KD}$ ECs revealed a pro-inflammatory phenotype with *CXCL1*, *CCL2* and *ICAM1* ranking as the top three upregulated genes in $CFTR^{KD}$ cells (supplementary table S4). CFTR-silenced ECs upregulated transcripts of various pro-inflammatory genes, adhesion molecules and TNF-related signalling (figure 5a). In baseline conditions and upon pro-inflammatory stimulus (lipopolysaccharide (LPS) challenge), $CFTR^{KD}$ ECs had a more pronounced pro-inflammatory phenotype than control cells, with elevated expression of *VCAM1*, *ICAM1*, *SELE* (E-selectin) and *IL8*. While LPS stimulation effectively increased the expression of activation markers in control ECs, it had no further effect on their already increased expression in $CFTR^{KD}$ ECs (figure 5b–e). Emerging evidence highlights that a loss in autophagy could contribute to EC activation [43]. However, rescuing the pro-inflammatory phenotype with rapamycin (an mTORC1 inhibitor inducing autophagy) did not alter the expression levels in either baseline or LPS challenge conditions (supplementary figure S4c). We hypothesised that increased expression of adhesion molecules and chemokines by ECs could result in more attraction and binding of leukocytes onto the EC surface. Therefore, we performed an *in vitro* leukocyte adhesion assay and confirmed that, compared to control ECs, more leukocytes adhered to the surface of CFTR-impaired ECs at both baseline and after LPS stimulation (figure 5f–i).

We then investigated the role of CFTR in a bi-transgenic mouse model of CFTR harbouring a targeted knockout ($CFTR^{KO}$) mutation of CFTR and expressing the human CFTR transgene under the expression of the *FABP1* promoter (rescuing the lethal intestinal occlusion phenotype occurring at birth [21]). Immunostaining of CD45, a marker of leukocytes, showed increased leukocyte infiltration into the lung and liver parenchyma of adult $CFTR^{KO}$ mice compared to wild-type littermates (figure 6a–d). Flow cytometry measurements of single-cell lung suspensions confirmed a heightened $CD45^+$ cell fraction and increased expression of VCAM1 and ICAM1 in viable $CD31^+$ $CD45^-$ cells isolated from $CFTR^{KO}$ mice (figure 6e–g, supplementary figure S4d). Our data thus suggest that across different model organisms, CFTR impairment leads to a pro-inflammatory phenotype in ECs, which can attract leukocytes and reinforce their extravasation across the endothelium.

CFTR mutations cause a pro-inflammatory phenotype in CF patient-derived ECs

In the clinical context that patients with CF can experience sustained periods of inflammation with an exaggerated immune response [44], we validated our findings in an *ex vivo* model using blood outgrowth endothelial cells (BOECs), cells derived from circulating EC progenitors that express typical EC markers [45]. BOECs were cultured from peripheral blood taken from CF patients with severe mutations (Class I–III; patients' clinical information is shown in supplementary table S1), and retained endothelial features when cultured *in vitro* (figure 7a, supplementary figure S4e). Confirming our previous results in HUVECs, wound closure and barrier integrity were also impaired in CF patient-derived BOECs (figure 7b, c). Similar to $CFTR^{KD}$ ECs, CF patient-derived BOECs displayed increased discontinuous and reticulated VE-cadherin junctions compared to BOECs from healthy donors (figure 7d–f). It has been suggested that such reticulated

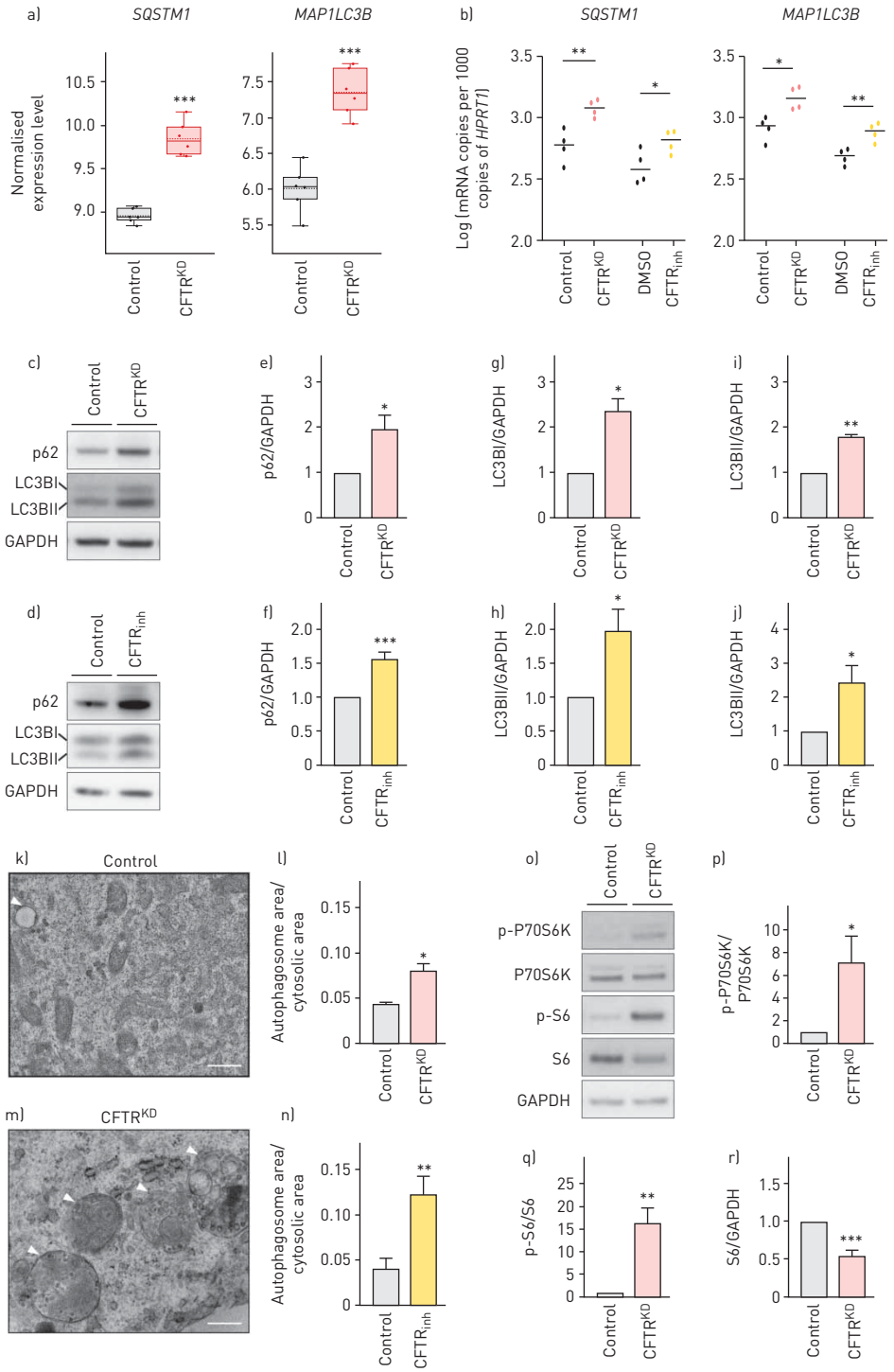

FIGURE 4 Autophagy defect in cystic fibrosis transmembrane conductance regulator (CFTR)-impaired endothelial cells (ECs). a) Boxplots showing normalised expression levels of *SQSTM1* and *MAP1LC3B* (encoding p62 and microtubule-associated protein 1 light chain 3B (LC3B), respectively) in ECs transduced with scrambled short hairpin RNA (shRNA) (control) and CFTR shRNA ($CFTR^{KD}$). n=6. ***: adjusted p<0.001 by moderated t-test. b) Quantitative reverse-transcriptase PCR analysis of *SQSTM1 and MAP1LC3B* expression levels in control and $CFTR^{KD}$ ECs, and DMSO-treated control *versus* CFTRinh-172-treated ($CFTR_{inh}$) ECs. Data are presented as individual data points with median; $CFTR^{KD}$ n=4; $CFTR_{inh}$ n=4. *: p<0.05; **: p<0.01 by two-tailed paired t-test. c–j) Representative immunoblots (c, d) and corresponding densitometric quantifications for p62 (e, f), LC3BI (g, h) and LC3BII (i, j) in control, $CFTR^{KD}$ or $CFTR_{inh}$ ECs. GAPDH was used as loading control. Data are presented as mean+SEM; $CFTR^{KD}$ n=4; $CFTR_{inh}$ n=8. *: p<0.05; **: p<0.01; ***: p<0.001 by one-sample t-test. k, m) Representative transmission electron microscopy of cultured control (k) *versus* $CFTR^{KD}$ (m) ECs indicates an accumulation of autophagosomes (white arrowheads). Scale bars: 500 nm. l, n) Quantification of autophagosome area for ECs upon $CFTR^{KD}$ (l) or $CFTR_{inh}$ (n). Data are presented as mean+SEM; $CFTR^{KD}$ n=3; $CFTR_{inh}$ n=4. *p<0.05; **p<0.01 by two-tailed paired t-test. o–r) Representative immunoblots and corresponding densitometric quantifications for p-P70S6K, P70S6K, p-S6 and S6 in control and $CFTR^{KD}$ ECs. GAPDH was used as loading control. Data are presented as mean+SEM. n=7. *: p<0.05; **: p<0.01; ***: p<0.001 by one-sample t-test.

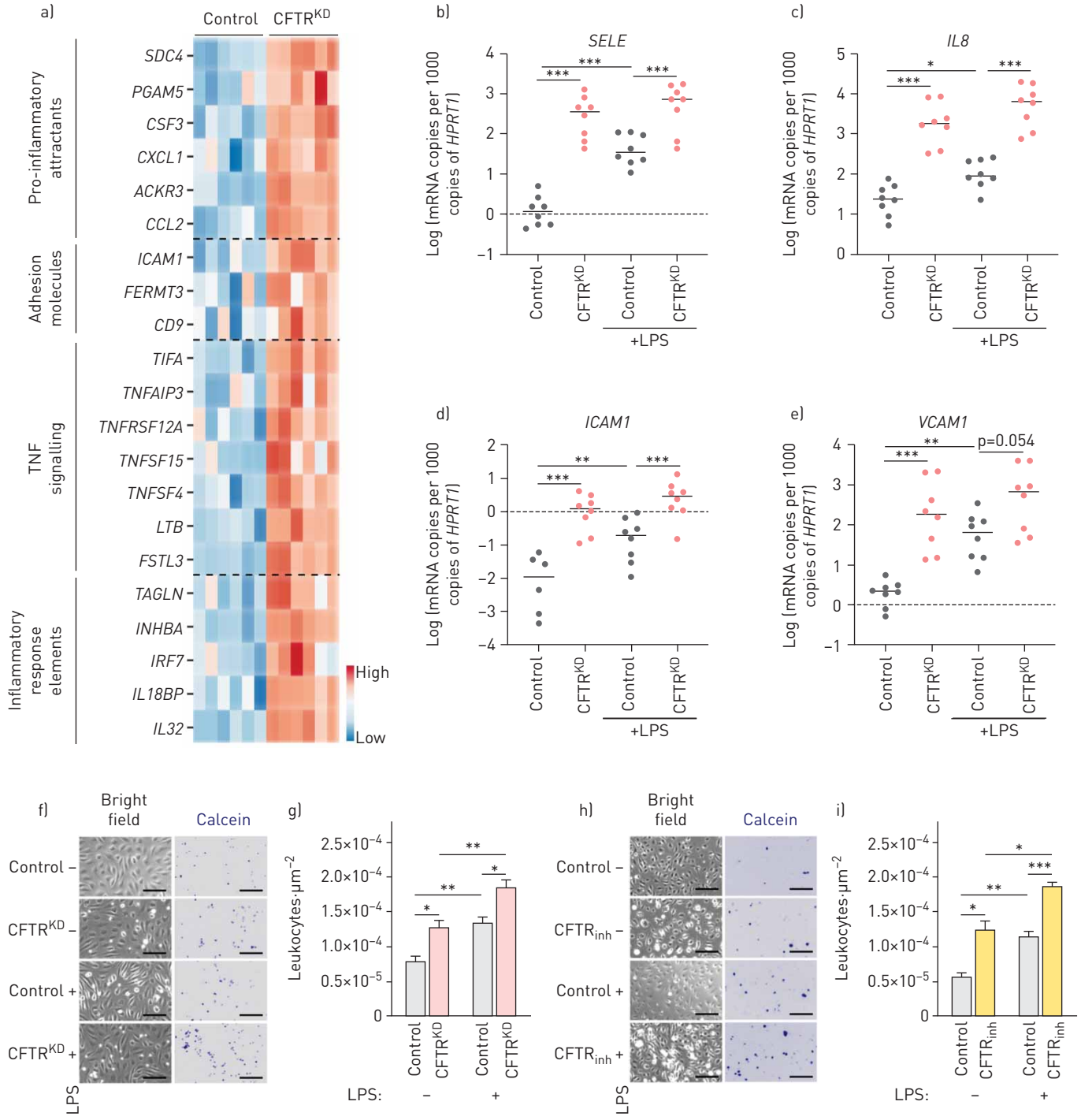

FIGURE 5 Cystic fibrosis transmembrane conductance regulator (CFTR) impairment induces endothelial cell (EC) activation. a) Heatmap showing the expression levels of differentially expressed genes between ECs transduced with scrambled short hairpin RNA (shRNA) (control) or CFTR shRNA ($CFTR^{KD}$). Selected genes are involved in inflammation and endothelial activation processes, and have adjusted p-values<0.05. Colour scale: red, high feature expression; blue, low feature expression. b–e) Quantitative reverse-transcriptase PCR analysis of *SELE* (b), *IL8* (c), *ICAM1* (d) and *VCAM1* (e) expression levels in control and $CFTR^{KD}$ ECs treated or not with lipopolysaccharide (LPS). Expression levels are normalised to *HPRT1*. Data are presented as individual data points with median; n⩾6. *: p<0.05; **: p<0.01; ***: p<0.001 by one-way ANOVA. f, h) Representative microscopy pictures of leukocyte adhesion assay to a monolayer of control and $CFTR^{KD}$ (f) or control and $CFTR_{inh}$ (h) ECs treated (+) or not (–) with LPS. Leukocytes are labelled with calcein (blue). Scale bars: 100 µm. g, i) Quantifications of leukocytes adhering to EC monolayers as shown in (f) and (h). Data are presented as mean+SEM; $CFTR^{KD}$ n=4; $CFTR_{inh}$ n=4. *: p<0.05; **: p<0.01; ***: p<0.001 by one-way ANOVA.

junctions are important in controlling leukocyte transmigration [37, 46, 47], corroborating the role of CFTR in barrier integrity and inflammation. Furthermore, mRNA levels of the pro-inflammatory *ICAM1*, *SELE* and *IL-8* were increased in BOECs from CF patients compared to healthy donors, which was mirrored in

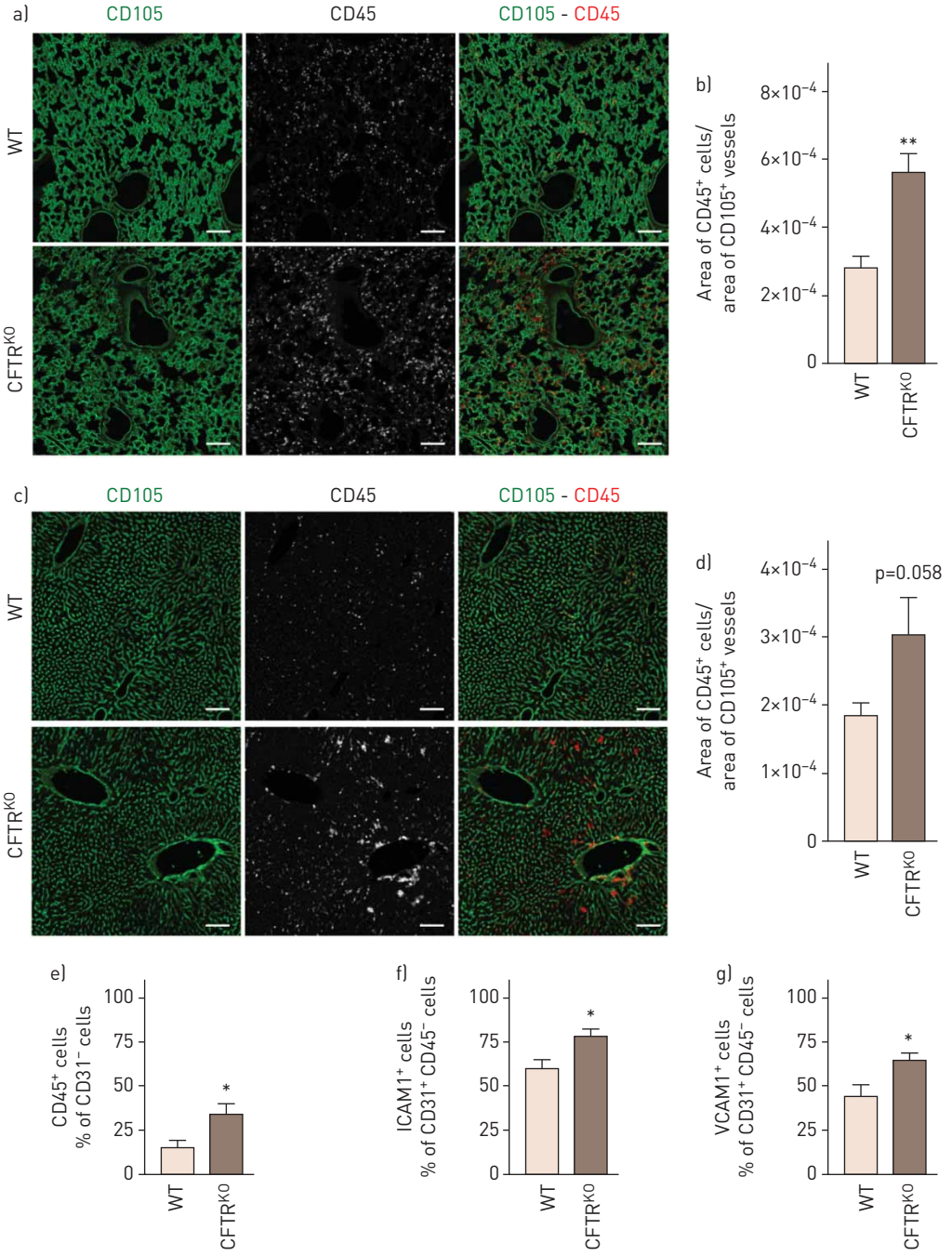

FIGURE 6 Cystic fibrosis transmembrane conductance regulator (CFTR) loss causes a pro-inflammatory phenotype *in vivo*. a, c) Representative confocal images of perfused lung (a) and liver (c) sections isolated from wild-type (WT) and $CFTR^{KO}$ littermates, stained for CD105 (vessels; green) and CD45 (leukocytes; red). Scale bars: 100 µm. b, d) Quantifications of CD45 area in perfused lung (b) and liver (d) sections. Data are presented as mean+SEM; n⩾4. **: p<0.01 by two-tailed unpaired t-test. e–g) Flow cytometry analysis of WT and $CFTR^{KO}$ mouse lung cell suspension for viable $CD45^+$ $CD31^-$ (e), $ICAM1^+$ $CD31^+$ $CD45^-$ (f) and $VCAM1^+$ $CD31^+$ $CD45^-$ (g) cells. Data are presented as mean+SEM; n⩾4. *: p<0.05 by two-tailed unpaired t-test.

the increased adherence of leukocytes to CF patient-derived ECs (figure 7g, h). These results correlate with our earlier findings, in which CFTR loss of function in our models resulted in a pro-inflammatory phenotype in ECs. More importantly, we found that rescuing CFTR function with the combination of CFTR modulators VX-770 and VX-809 (Orkambi®) was also able to partially rescue the pro-inflammatory gene expression signature, and significantly diminished leukocyte adhesion onto CF patient-derived ECs (figure 7h, i).

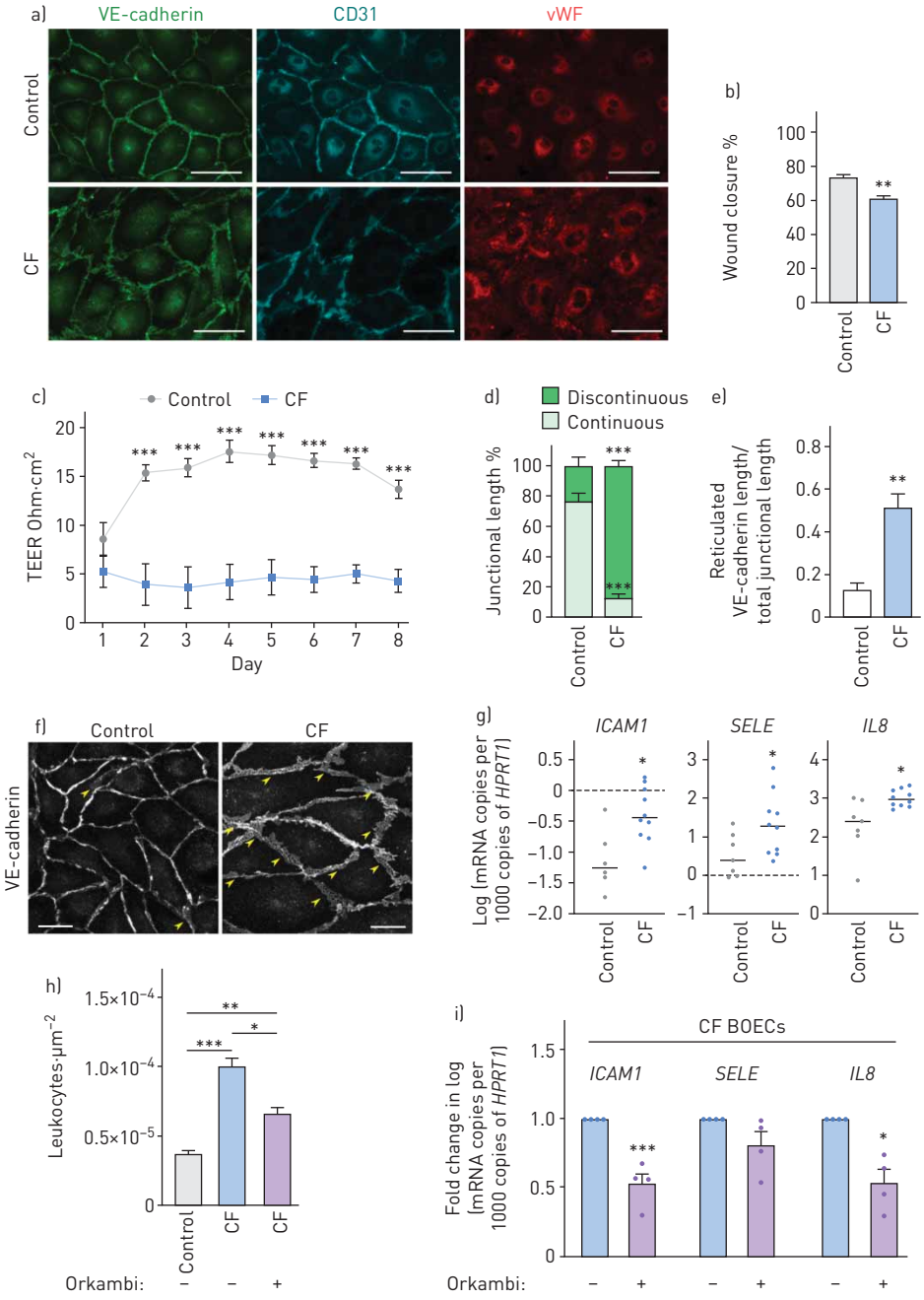

FIGURE 7 In cystic fibrosis (CF) patients, cystic fibrosis transmembrane conductance regulator (CFTR) loss promotes endothelial cell (EC) dysfunction and activation. a) Representative confocal images of blood outgrowth endothelial cells (BOECs) from healthy donors (control) and CF patients stained for vascular endothelial cadherin (VE-cadherin), CD31 and von Willebrand factor (vWF). Scale bar: 50 µm. b) Scratch wound migration assay with control and CF BOECs (n=3). Data are presented as mean+SEM. **: p<0.01 by two-tailed unpaired t-test. c) Trans-endothelial electrical resistance (TEER) assay with control and CF BOECs (n=6). Data are presented as mean±SEM. ***: p<0.001 by two-way ANOVA. d, e) Quantification of the fraction of discontinuous and continuous VE-cadherin-stained junctions (d), and the fraction of reticulated VE-cadherin junctions (e) in control and CF BOEC monolayers (n=4). Data are presented as mean+SEM. **: p<0.01; ***: p<0.001 by two-tailed unpaired t-test. f) Representative confocal images of reticulated adherens junctions in control and CF patient-derived BOEC monolayers stained for VE-cadherin. Yellow arrowheads indicate discontinuous junctions. Scale bar: 25 µm. g) Quantitative reverse-transcriptase (qRT)-PCR analysis of *ICAM1*, *SELE* and *IL8* expression levels in control and CF BOECs. Expression levels are normalised to *HPRT1*. Data are presented as individual data points with median; n⩾6. *: p<0.05 by two-tailed unpaired t-test. h) Quantification of leukocytes adhering to control and CF BOEC monolayers, treated or not with the Orkambi CFTR modulators combination (VX-770 and VX-809) (n=3). Data are presented as mean+SEM. *: p<0.05; **: p<0.01; ***: p<0.001 by one-way ANOVA. i) qRT-PCR analysis of *ICAM1*, *SELE* and *IL8* expression levels in BOECs from CF patients treated or not with Orkambi. Expression levels are normalised to *HPRT1*. Data are presented as bar plots and individual data points with mean+SEM; n=4. *: p<0.05; ***: p<0.001 by two-tailed paired t-test.

Discussion

Inflammation plays a major role in CF pathophysiology, in which it affects mainly the lungs but also organs such as the liver, intestines and pancreas [2]. The origin of the inflammation in CF-affected organs is currently debated because it is unclear whether it is of primary or secondary origin [4, 48]. A pro-inflammatory phenotype has been observed in different cell types independent of pro-inflammatory challenges [49–51], *e.g.* in HUVECs treated with CFTR inhibitor, which produced more IL-8 [39, 52]. Our bulk transcriptomic data revealed upregulated expression of multiple pro-inflammatory genes in CFTR-impaired ECs. Upon CFTR impairment *in vitro* and in CF patient-derived ECs *ex vivo*, the expression of several EC pro-inflammatory genes (*ICAM1*, *IL-8* and *SELE*), which are essential molecules for leukocyte adhesion and diapedesis, was upregulated. This was mirrored by increased leukocyte adhesion to CFTR-impaired ECs. These findings confirm that CFTR dysfunction by itself leads to a pro-inflammatory phenotype even in the absence of a concomitant infection. CFTR-modulator treatment has already been successfully used to rescue CFTR function in other *in vitro* systems, even showing clinical correlation to patient response [53, 54]. Accordingly, the combination treatment of VX-770 and VX-809 (Orkambi®) was able to partially rescue the pro-inflammatory phenotype of CF patient-derived ECs, as measured by inflammatory marker gene expression and leukocyte adhesion. Our results are in accordance with earlier findings in CF patients in which increased soluble EC activation molecules were detected in the plasma and serum, correlating, in some cases, with impaired lung function [55–60]. Additionally, in the gut-corrected $CFTR^{KO}$ mouse model, microscopic quantifications revealed more leukocyte infiltration in lung and liver, with increased expression of leukocyte adhesion molecules in lung ECs. Although these $CFTR^{KO}$ mice do not display the inflammatory lung phenotype [20, 61], they do show signs of subsymptomatic inflammation, for which the vasculature could thus at least be partly responsible by promoting leukocyte adhesion and infiltration. Hence, CFTR impairment leads to an inflammatory EC phenotype with increased activation and leukocyte extravasation, highlighting the potential, but overlooked role of the endothelium as a mediator in the inflammatory process in CF. In support of a role of ECs in immune regulation, we recently observed that freshly isolated tumour ECs from human lung cancers expressed a transcriptome signature associated with diverse immune functions, suggesting a more important function of disease ECs in immune surveillance than previously anticipated [62].

We propose that three potential interlinked underlying mechanisms give rise to this increase in inflammation: 1) defective autophagy, 2) increased oxidative stress and 3) mitochondrial dysfunction (figure 8). Our study provides several lines of evidence that autophagy might be defective in ECs with impaired CFTR function. We observed increased protein levels of the autophagy marker LC3BI, thus confirming autophagy induction. However, analysis of autophagic flux using LC3BII and TEM images revealed autophagosome accumulation, indicating decreased autophagic flux due to defective autophagosome maturation and/or autolysosome function. Although an autophagy impairment has been reported in CF-deficient epithelial cells and macrophages, in which accumulation of p62 is documented together with a decrease in LC3BII and autophagosomes [63, 64], our mechanism seems to be distinct because it is characterised by an accumulation of autophagosomes. Autophagy is a highly dynamic process with several components and mediators involved, including mTORC1, a key regulator of autophagosome formation and lysosome biogenesis [65]. We observed increased mTORC1 activity in $CFTR^{KD}$ ECs, suggesting inhibition of autophagy. Indeed, a prominent function of mTORC1 is to restrict autophagy [42]; however, reactivation of mTORC1 is required for the termination of autophagy [66]. Defective autophagy has already been associated with a pro-inflammatory phenotype in different cell types, including ECs [67, 68], and could contribute to the pro-inflammatory phenotype in CF. In addition, it is well established that impaired cellular proteostasis and autophagy are involved in the pathogenesis of CF [69]. In fact, correcting the underlying proteostasis and autophagy defect has emerged as a novel intervention strategy in CF [69].

Increased oxidative stress is another hallmark of CF pathophysiology [40]. We observed increased oxidative stress in CFTR-impaired ECs, together with a striking transcriptomic signature in which multiple antioxidant-related genes were upregulated. Although our data revealed that the rate-controlling enzyme for GSH synthesis (a key intracellular antioxidant) was unchanged upon CFTR silencing, glutathione disulfide (GSSG) and $NADP^+$ levels were increased, suggesting increased oxidative stress. Our findings confirm earlier studies in CF patients that documented heightened vascular oxidative stress, probably scavenging the vasodilator nitric oxide (NO), leading to reduced NO bioavailability, EC activation and dysfunction [70–72]. The role of excessive ROS levels in the respiratory system has mostly been characterised in connection with chronic pulmonary infections and persistent inflammation [40]. Additionally, low GSH levels have been found in plasma and blood neutrophils from CF patients [73, 74] and systemic GSH dyshomeostasis has already been suggested in CF [40]. Because of the heightened oxidative stress in CF patients, CF research has also explored the potential of antioxidant treatment [40, 75]. Recently, an antioxidant cocktail treatment in CF patients improved both vascular and lung function [71].

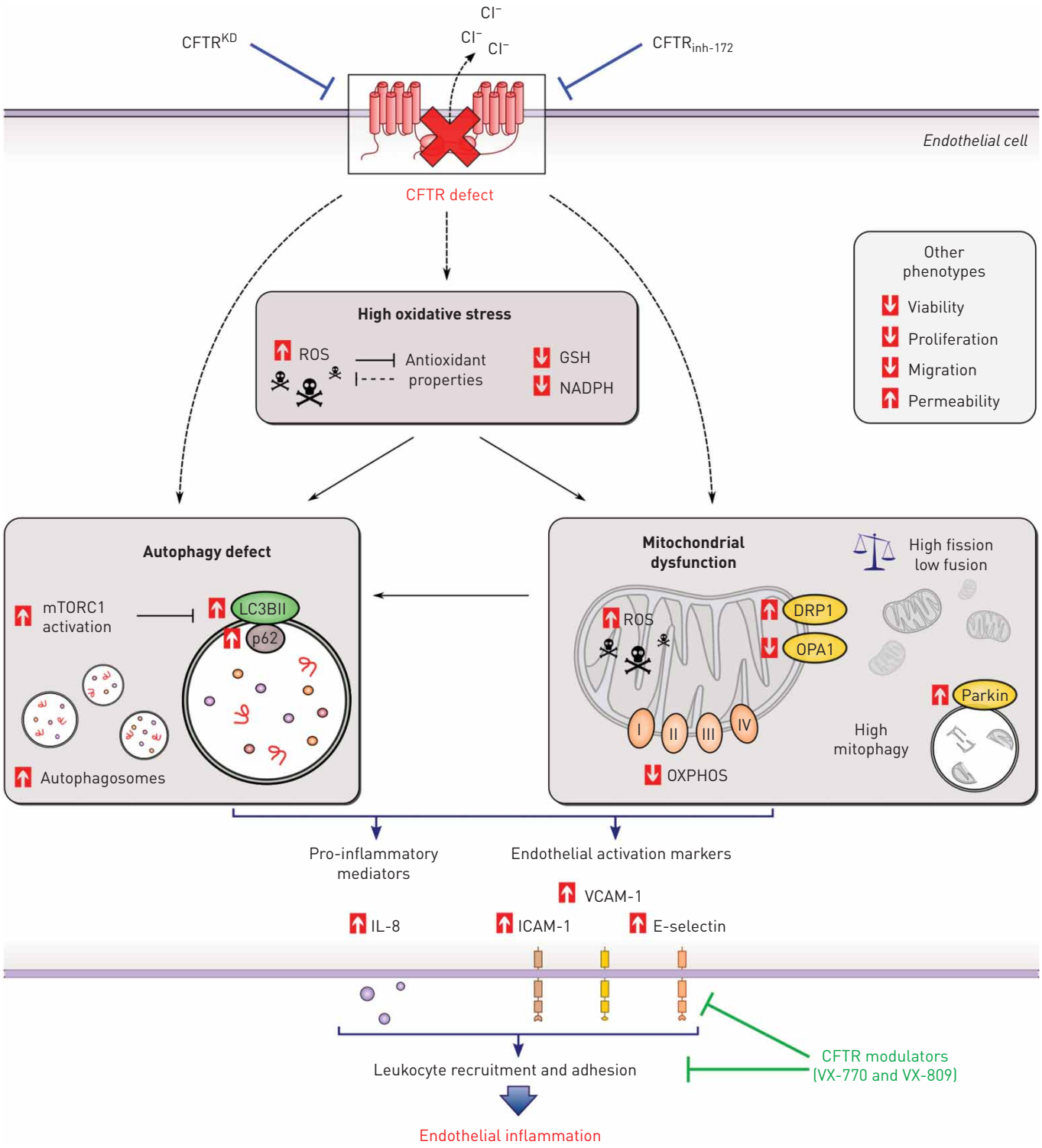

FIGURE 8 Summary of key events occurring in endothelial cells (ECs) upon cystic fibrosis transmembrane conductance regulator (CFTR) impairment. Upon endothelial CFTR impairment, three potential interlinked underlying mechanisms could give rise to the increase in endothelial activation and subsequent heightened inflammation: 1) increased oxidative stress and decreased antioxidant properties, 2) defective autophagy characterised by autophagosome accumulation and 3) mitochondrial dysfunction. Other observed EC phenotypes included decreased viability (when CFTR expression level/activity was almost completely abolished), proliferation and wound closure, and increased membrane permeability. $CFTR^{KD}$: CFTR short hairpin RNA; $CFTR_{inh}$: CFTRinh-172; ROS: reactive oxygen species; GSH: glutathione; mTORC1: mammalian target of rapamycin complex 1; LC3B: microtubule-associated protein 1 light chain 3B; DRP1: dynamin related protein 1; OPA1: OPA1 mitochondrial dynamin like GTPase; OXPHOS: oxidative phosphorylation; IL-8: interleukin 8; VCAM-1: vascular cell adhesion molecule 1; ICAM-1: intercellular adhesion molecule 1.

Although these results are promising, the beneficial effect of antioxidant therapy remains difficult to evaluate in CF patients with chronic infections on intensive antibiotic treatments and warrants a large-scale, long-term study [75].

Mitochondria can be ROS-producing organelles and CFTR function is necessary for optimal mitochondrial function [76, 77]. We consistently found increased mitochondrial ROS in CFTR-impaired ECs. A previous study in human bronchial epithelial cells reported that oxygen consumption and both mitochondrial complex I and IV activities were impaired in CF epithelial cells, concomitantly associated with increased mitochondrial ROS production and membrane lipid peroxidation [78]. We confirmed these findings in ECs, finding that both basal and maximal respiration as well as mitochondrial ATP production were decreased in CFTR-impaired ECs. Currently, the molecular mechanisms explaining how CFTR impairment affects so many parameters of mitochondrial function remain unknown [78]. In the absence of efficient removal of damaged mitochondria (mitophagy), ROS levels would be expected to rise. Our observations of increased mitochondrial fission and impaired mitophagy suggest that increased mitochondrial damage is at least partly responsible for the observed mitochondrial phenotype. However, we cannot conclude which mechanism is initiating the mitochondriopathy: (mitochondrial) ROS inducing autophagy/mitophagy or *vice versa* (figure 8). The process of autophagy/mitophagy in ECs might be particularly important in CF because impairment of this pathway contributes to inflammasome activation [67, 79].

From our transcriptomics data, we observed downregulation of essential marker genes for proliferation, as well as cyclins and cyclin-dependent kinases [80], consistent with our functional validation *in vitro*. The mechanisms by which chloride fluxes are affecting interactions between cyclins and cyclin-dependent kinases, thereby regulating cell cycle, are poorly characterised, especially in ECs. Although interesting, how and if an EC proliferation defect might contribute to CF disease progression is currently unknown.

EC migration is a regulated multistep process involved in tissue formation, wound healing and regeneration [81]. Upon CFTR impairment, ECs exhibited decreased migration, which is in accordance with their transcriptomic signature. We also obtained evidence that CFTR is expressed at the lamellipodia of migrating ECs and therefore is possibly involved in EC polarisation and migration. Our findings are consistent with reports that CFTR regulates lamellipodia protrusion and cell migration in non-EC types [82, 83]. It is becoming increasingly obvious that CFTR regulates cell migration across a diverse range of cell types; however, the underlying mechanisms remain to be elucidated, given that delayed wound repair may augment inflammation in CF [82].

The endothelium also functions as a semipermeable barrier where EC junctions dynamically open to allow the passage of ions, nutrients and inflammatory cells for tissue homeostasis and immune surveillance. In accordance with published literature [38, 39], we observed increased membrane permeability in $CFTR^{KD}$ cells and CF patient-derived ECs. This was probably caused by the larger number of discontinuous junctions present when CFTR was impaired. More interestingly, $CFTR^{KD}$ cells and CF patient-derived ECs displayed higher fractions of reticulated adherens junctions. Such reticulated junctions are important in controlling leukocyte transmigration [37, 46, 47]. This reinforces our hypothesis that CFTR impairment is associated with a pro-inflammatory and leaky barrier, which could possibly contribute to the excessive leukocyte extravasation observed in the lung of CF patients [84].

Our study has limitations and outstanding questions. For instance, how does CFTR, a protein in the plasma membrane that regulates ion conductivity, regulate diverse processes such as endothelial proliferation, migration, autophagy and inflammation? It is well known that CFTR is a promiscuous protein that also functions as a protein hub for scaffolding proteins at the plasma membrane and in the Golgi apparatus [85–87]. Protein–protein interactome analysis revealed that CFTR is involved in a wide range of processes (including proteostasis, cytoskeleton remodelling, immune response, ROS signalling, metabolism and proliferation), highlighting the complex underlying regulatory network [88]. Limitations to our study are the low endogenous CFTR levels in ECs, making its detection challenging, and the fact that we had to use a limited $CFTR^{KD}$ efficiency to avoid cellular toxicity at higher $CFTR^{KD}$ efficiency. However, this incomplete $CFTR^{KD}$ was sufficient to induce the observed vascular inflammation and other phenotypes, indicating its physiological relevance. It was thought that CF carriers (50% CFTR expression) could remain healthy [89, 90]; however, it was recently observed that CF carriers have increased risk for a wide range of CF-related conditions [91]. Thus, studying and comparing carrier- *versus* CF patient-derived ECs would give insightful information. It is well established that gut-corrected $CFTR^{KO}$ mice are not an ideal model organism to study CF because this model does not accurately reflect the human phenotype [20, 61]. Given that CFTR is absent in almost all cell types, other cell types could also influence the increased leukocyte extravasation found in murine CF lungs. However, endothelial leukocyte adhesion markers were increased in murine $CFTR^{KO}$ lung ECs, suggesting that the endothelium could partially mediate the excessive extravasation. Obtaining primary ECs from CF patients is challenging. We therefore

used BOECs as an alternative, though the extent to which these cells reflect *in situ* organ-derived ECs from CF patients needs studying. Nevertheless, we observed a similar pro-inflammatory signature in BOECs from CF patients as in ECs with impaired CFTR function.

In conclusion, our findings provide new evidence that EC function is altered upon CFTR impairment, with defective cell proliferation, migration and autophagy. Remarkably, altered CFTR expression led to EC activation and a pro-inflammatory state, increasing leukocyte adhesion and extravasation *in vitro*, *in vivo* and *ex vivo*. Our data raise the question of whether ECs should still be considered as passive bystanders in CF pathology, or whether they actively co-determine the exaggerated inflammatory response. Hence, our study may provide an incentive to consider EC normalisation as a new therapeutic approach to reduce the pro-inflammatory status of ECs and thereby improve the quality of life of CF patients.

Acknowledgements: The authors thank P. Agostinis and A. Luttun for discussion and advice. They also thank M. Parys, S. Wyns, C. De Legher, J. Souffreau, I. Betz, P. Vanwesemael, B. Verherstraeten, A. Manderveld, A. Carton, K. Peeters, N. Dai, L. De Keersmaecker and W. Vermaelen for technical assistance. We thank the Genomics Core Leuven for the RNA sequencing. The authors would like to thank the CF patients and hospital staff of the UZ Leuven CF centre who participated in this study.

Author contributions: M. Declercq, L. Treps, P. Carmeliet, D. Cassiman and P. Witters designed the research. M. Declercq, L. Treps, P. de Zeeuw, M. García-Caballero, K. Brepoels, S. Vinckier and B. Ghesquière performed the research. P. de Zeeuw, N. Vasconcelos Conchinha, V. Geldhof, M. Ensinck, M.S. Carlon, A.S. Ramalho, M.J. Bird, M. Proesmans, F. Vermeulen, L. Dupont, B. Ghesquière, G. Eelen and M. Dewerchin contributed vital new reagents or analytic tools. M. Declercq, L. Treps, P. Carmeliet and P. Witters analysed data. M. Declercq, L. Treps, P. Carmeliet and P. Witters wrote the paper. All authors discussed the results and commented on the manuscript.

Conflict of interest: None declared.

Support statement: M. Declercq and P. Witters are funded by the King Baudouin Foundation, Mucovereniging and UZ Leuven. L. Treps and M.S. Carlon are funded by an FWO Fellowship. P. Carmeliet is supported by the long-term structural Methusalem funding by the Flemish Government, grants from the Research Foundation Flanders (FWO-Vlaanderen), an ERC Proof of Concept Grant and an ERC Advanced Grant. Funding information for this article has been deposited with the Crossref Funder Registry.

References

1 Ratjen F, Bell SC, Rowe SM, *et al.* Cystic fibrosis. *Nat Rev Dis Prim* 2015; 1: 15010.
2 Cutting GR. Cystic fibrosis genetics: from molecular understanding to clinical application. *Nat Rev Genet* 2015; 16: 45–56.
3 Stoltz DA, Rokhlina T, Ernst SE, *et al.* Intestinal CFTR expression alleviates meconium ileus in cystic fibrosis pigs. *J Clin Invest* 2013; 123: 2685–2693.
4 Cantin AM, Hartl D, Konstan MW, *et al.* Inflammation in cystic fibrosis lung disease: pathogenesis and therapy. *J Cyst Fibros* 2015; 14: 419–430.
5 Galley HF, Webster NR. Physiology of the endothelium. *Br J Anaesth* 2004; 93: 105–113.
6 Rajendran P, Rengarajan T, Thangavel J, *et al.* The vascular endothelium and human diseases. *Int J Biol Sci* 2013; 9: 1057–1069.
7 Tousson A, Van Tine BA, Naren AP, *et al.* Characterization of CFTR expression and chloride channel activity in human endothelia. *Am J Physiol* 1998; 275: C1555–C1564.
8 Sun XC, Zhai C-B, Cui M, *et al.* HCO-3-dependent soluble adenylyl cyclase activates cystic fibrosis transmembrane conductance regulator in corneal endothelium. *Am J Physiol Cell Physiol* 2003; 284: C1114–C1122.
9 Poore S, Berry B, Eidson D, *et al.* Evidence of vascular endothelial dysfunction in young patients with cystic fibrosis. *Chest* 2013; 143: 939–945.
10 Rodriguez-Miguelez P, Thomas J, Seigler N, *et al.* Evidence of microvascular dysfunction in patients with cystic fibrosis. *Am J Physiol Hear Circ Physiol* 2016; 310: 1479–1485.
11 Reverri EJ, Morrissey BM, Cross CE, *et al.* Inflammation, oxidative stress, and cardiovascular disease risk factors in adults with cystic fibrosis. *Free Radic Biol Med* 2014; 76: 261–277.
12 Declercq M, Treps L, Carmeliet P, *et al.* The role of endothelial cells in cystic fibrosis. *J Cyst Fibros* 2019; 18: 752–761.
13 Vasan RS, Larson MG, Aragam J, *et al.* Genome-wide association of echocardiographic dimensions, brachial artery endothelial function and treadmill exercise responses in the Framingham Heart Study. *BMC Med Genet* 2007; 8: 1–14.
14 van der Harst P, Verweij N. Identification of 64 novel genetic loci provides an expanded view on the genetic architecture of coronary artery disease. *Circ Res* 2018; 122: 433–443.
15 De Bock K, Georgiadou M, Schoors S, *et al.* Role of PFKFB3-driven glycolysis in vessel sprouting. *Cell* 2013; 154: 651–663.
16 Schoors S, Bruning U, Missiaen R, *et al.* Fatty acid carbon is essential for dNTP synthesis in endothelial cells. *Nature* 2015; 520: 192–197.
17 Martin-Ramirez J, Hofman M, van den Biggelaar M, *et al.* Establishment of outgrowth endothelial cells from peripheral blood. *Nat Protoc* 2012; 7: 1709–1715.
18 Eelen G, Dubois C, Cantelmo AR, *et al.* Role of glutamine synthetase in angiogenesis beyond glutamine synthesis. *Nature* 2018; 561: 63–69.
19 Kalucka J, Bierhansl L, Conchinha NV, *et al.* Quiescent endothelial cells upregulate fatty acid β-oxidation for vasculoprotection via redox homeostasis. *Cell Metab* 2018; 28: 881–894.

20 Munder A, Wölbeling F, Kerber-Momot T, *et al.* Acute intratracheal *Pseudomonas aeruginosa* infection in cystic fibrosis mice is age-independent. *Respir Res* 2011; 12: 148.
21 Zhou L, Dey CR, Wert SE, *et al.* Correction of lethal intestinal defect in a mouse model of cystic fibrosis by human CFTR. *Science* 1994; 266: 1705–1708.
22 Andrews S. FastQC: a quality control tool for high throughput sequence data. 2010. www.bioinformatics.babraham.ac.uk/projects/fastqc/. Date last accessed:
23 Huang H, Vandekeere S, Kalucka J, *et al.* Role of glutamine and interlinked asparagine metabolism in vessel formation. *EMBO J* 2017; 36: 2334–2352.
24 Wong BW, Wang X, Zecchin A, *et al.* The role of fatty acid β-oxidation in lymphangiogenesis. *Nature* 2017; 542: 49–54.
25 Veys K, Fan Z, Ghobrial M, *et al.* Role of the GLUT1 glucose transporter in postnatal CNS angiogenesis and blood–brain barrier integrity. *Circ Res* 2020; 127: 466–482.
26 García-Caballero M, Zecchin A, Souffreau J, *et al.* Role and therapeutic potential of dietary ketone bodies in lymph vessel growth. *Nat Metab* 2019; 1: 666–675.
27 Vandekeere S, Dubois C, Kalucka J, *et al.* Serine synthesis via PHGDH is essential for heme production in endothelial cells. *Cell Metab* 2018; 28: 573–587.
28 Taverna F, Goveia J, Karakach TK, *et al.* BIOMEX: an interactive workflow for (single cell) omics data interpretation and visualization. *Nucleic Acids Res* 2020; 48: W385–W394.
29 De Boeck K, Amaral MD. Progress in therapies for cystic fibrosis. *Lancet Respir Med* 2016; 4: 662–674.
30 Melis N, Tauc M, Cougnon M, *et al.* Revisiting CFTR inhibition: a comparative study of CFTRinh-172 and GlyH-101 inhibitors. *Br J Pharmacol* 2014; 171: 3716–3727.
31 Subramanian A, Tamayo P, Mootha VK, *et al.* Gene set enrichment analysis: a knowledge-based approach for interpreting genome-wide expression profiles. *Proc Natl Acad Sci USA* 2005; 102: 15545–15550.
32 Reyes R, Cardeñes B, Machado-Pineda Y, *et al.* Tetraspanin CD9: a key regulator of cell adhesion in the immune system. *Front Immunol* 2018; 9: 863.
33 Imhof BA, Jemelin S, Ballet R, *et al.* CCN1/CYR61-mediated meticulous patrolling by Ly6C^{low} monocytes fuels vascular inflammation. *Proc Natl Acad Sci USA* 2016; 113: E4847–E4856.
34 Hardy LA, Booth TA, Lau EK, *et al.* Examination of MCP-1 (CCL2) partitioning and presentation during transendothelial leukocyte migration. *Lab Investig* 2004; 84: 81–90.
35 Girbl T, Lenn T, Perez L, *et al.* Distinct compartmentalization of the chemokines CXCL1 and CXCL2 and the atypical receptor ACKR1 determine discrete stages of neutrophil diapedesis. *Immunity* 2018; 49: 1062–1076.
36 Fraccaroli A, Pitter B, Taha AA, *et al.* Endothelial α-parvin controls integrity of developing vasculature and is required for maintenance of cell-cell junctions. *Circ Res* 2015; 117: 29–40.
37 Fernández-Martín L, Marcos-Ramiro B, Bigarella CL, *et al.* Crosstalk between reticular adherens junctions and platelet endothelial cell adhesion molecule-1 regulates endothelial barrier function. *Arterioscler Thromb Vasc Biol* 2012; 32: e90–e102.
38 Brown MB, Hunt WR, Noe JE, *et al.* Loss of cystic fibrosis transmembrane conductance regulator impairs lung endothelial cell barrier function and increases susceptibility to microvascular damage from cigarette smoke. *Pulm Circ* 2014; 4: 260–268.
39 Totani L, Plebani R, Piccoli A, *et al.* Mechanisms of endothelial cell dysfunction in cystic fibrosis. *Biochim Biophys Acta Mol Basis Dis* 2017; 1863: 3243–3253.
40 Galli F, Battistoni A, Gambari R, *et al.* Oxidative stress and antioxidant therapy in cystic fibrosis. *Biochim Biophys Acta Mol Basis Dis* 2012; 1822: 690–713.
41 Palikaras K, Lionaki E, Tavernarakis N. Mechanisms of mitophagy in cellular homeostasis, physiology and pathology. *Nat Cell Biol* 2018; 20: 1013–1022.
42 Kim J, Guan K-L. mTOR as a central hub of nutrient signalling and cell growth. *Nat Cell Biol* 2019; 21: 63–71.
43 Schaaf MB, Houbaert D, Meçe O, *et al.* Autophagy in endothelial cells and tumor angiogenesis. *Cell Death Differ* 2019; 26: 665–679.
44 Ratner D, Mueller C. Immune responses in cystic fibrosis. *Am J Respir Cell Mol Biol* 2012; 46: 715–722.
45 Lin Y, Weisdorf DJ, Solovey A, *et al.* Origins of circulating endothelial cells and endothelial outgrowth from blood. *J Clin Invest* 2000; 105: 71–77.
46 Muller WA, Weigl SA, Deng X, *et al.* PECAM-1 is required for transendothelial migration of leukocytes. *J Exp Med* 1993; 178: 449–460.
47 Carman C V, Springer TA. A transmigratory cup in leukocyte diapedesis both through individual vascular endothelial cells and between them. *J Cell Biol* 2004; 167: 377–388.
48 Stoltz DA, Meyerholz DK, Welsh MJ. Origins of cystic fibrosis lung disease. *N Engl J Med* 2015; 372: 351–362.
49 Perez A, Issler AC, Cotton CU, *et al.* CFTR inhibition mimics the cystic fibrosis inflammatory profile. *Am J Physiol Cell Mol Physiol* 2007; 292: L383–L395.
50 Fiorotto R, Scirpo R, Trauner M, *et al.* Loss of CFTR affects biliary epithelium innate immunity and causes TLR4-NF-κB-mediated inflammatory response in mice. *Gastroenterology* 2011; 141: 1498–1508.
51 Crites KS-M, Morin G, Orlando V, *et al.* CFTR knockdown induces proinflammatory changes in intestinal epithelial cells. *J Inflamm* 2015; 12: 62.
52 Khalaf M, Scott-Ward T, Causer A, *et al.* Cystic fibrosis transmembrane conductance regulator (CFTR) in human lung microvascular endothelial cells controls oxidative stress, reactive oxygen-mediated cell signaling and inflammatory responses. *Front Physiol* 2020; 11: 879.
53 Dekkers JF, Wiegerinck CL, de Jonge HR, *et al.* A functional CFTR assay using primary cystic fibrosis intestinal organoids. *Nat Med* 2013; 19: 939–945.
54 Berkers G, van Mourik P, Vonk AM, *et al.* Rectal organoids enable personalized treatment of cystic fibrosis. *Cell Rep* 2019; 26: 1701–1708.
55 Watts KD, McColley SA. Elevated vascular endothelial growth factor is correlated with elevated erythropoietin in stable, young cystic fibrosis patients. *Pediatr Pulmonol* 2011; 46: 683–687.
56 Dufresne V, Knoop C, Van Muylem A, *et al.* Effect of systemic inflammation on inspiratory and limb muscle strength and bulk in cystic fibrosis. *Am J Respir Crit Care Med* 2009; 180: 153–158.

57 De Rose V, Oliva A, Messore B, *et al.* Circulating adhesion molecules in cystic fibrosis. *Am J Respir Crit Care Med* 1998; 157: 1234–1239.
58 Romano M, Collura M, Iapichino L, *et al.* Endothelial perturbation in cystic fibrosis. *Thromb Haemost* 2001; 86: 1363–1367.
59 Sturm A, Hebestreit H, Koenig C, *et al.* Platelet proinflammatory activity in clinically stable patients with CF starts in early childhood. *J Cyst Fibros* 2010; 9: 179–186.
60 Nowak JK, Wojsyk-Banaszak I, Mądry E, *et al.* Increased soluble VCAM-1 and normal P-selectin in cystic fibrosis: a cross-sectional study. *Lung* 2017; 195: 445–453.
61 Zhou L, Dey CR, Wert SE, *et al.* Correction of lethal intestinal defect in a mouse model of cystic fibrosis by human CFTR. *Science* 1994; 266: 1705–1708.
62 Goveia J, Rohlenova K, Taverna F, *et al.* An integrated gene expression landscape profiling approach to identify lung tumor endothelial cell heterogeneity and angiogenic candidates. *Cancer Cell* 2020; 37: 21–36.e13.
63 Luciani A, Villella VR, Esposito S, *et al.* Defective CFTR induces aggresome formation and lung inflammation in cystic fibrosis through ROS-mediated autophagy inhibition. *Nat Cell Biol* 2010; 12: 863–875.
64 Abdulrahman BA, Khweek AA, Akhter A, *et al.* Autophagy stimulation by rapamycin suppresses lung inflammation and infection by *Burkholderia cenocepacia* in a model of cystic fibrosis. *Autophagy* 2011; 7: 1359–1370.
65 Dossou SA, Basu A. The emerging roles of mTORC1 in macromanaging autophagy. *Cancers* 2019; 11: 1422.
66 Yu L, McPhee CK, Zheng L, *et al.* Termination of autophagy and reformation of lysosomes regulated by mTOR. *Nature* 2010; 465: 942–946.
67 Netea-Maier RT, Plantinga TS, van de Veerdonk FL, *et al.* Modulation of inflammation by autophagy: consequences for human disease. *Autophagy* 2016; 12: 245–260.
68 Vion A-C, Kheloufi M, Hammoutene A, *et al.* Autophagy is required for endothelial cell alignment and atheroprotection under physiological blood flow. *Proc Natl Acad Sci USA* 2017; 114: E8675–E8684.
69 Bodas M, Vij N. Adapting proteostasis and autophagy for controlling the pathogenesis of cystic fibrosis lung disease. *Front Pharmacol* 2019; 10: 20.
70 Tucker MA, Berry B, Seigler N, *et al.* Blood flow regulation and oxidative stress during submaximal cycling exercise in patients with cystic fibrosis. *J Cyst Fibros* 2018; 17: 256–263.
71 Tucker MA, Fox BM, Seigler N, *et al.* Endothelial dysfunction in cystic fibrosis: role of oxidative stress. *Oxid Med Cell Longev* 2019; 2019: 1629638.
72 Incalza MA, D'Oria R, Natalicchio A, *et al.* Oxidative stress and reactive oxygen species in endothelial dysfunction associated with cardiovascular and metabolic diseases. *Vascul Pharmacol* 2018; 100: 1–19.
73 Roum JH, Buhl R, McElvaney NG, *et al.* Systemic deficiency of glutathione in cystic fibrosis. *J Appl Physiol* 1993; 75: 2419–2424.
74 Tirouvanziam R, Conrad CK, Bottiglieri T, *et al.* High-dose oral N-acetylcysteine, a glutathione prodrug, modulates inflammation in cystic fibrosis. *Proc Natl Acad Sci USA* 2006; 103: 4628–4633.
75 Ciofu O, Smith S, Lykkesfeldt J. Antioxidant supplementation for lung disease in cystic fibrosis. *Cochrane Database Syst Rev* 2019; 10: CD007020.
76 Valdivieso AG, Santa-Coloma TA. CFTR activity and mitochondrial function. *Redox Biol* 2013; 1: 190–202.
77 Favia M, de Bari L, Bobba A, *et al.* An intriguing involvement of mitochondria in cystic fibrosis. *J Clin Med* 2019; 8: 1890.
78 Atlante A, Favia M, Bobba A, *et al.* Characterization of mitochondrial function in cells with impaired cystic fibrosis transmembrane conductance regulator (CFTR) function. *J Bioenerg Biomembr* 2016; 48: 197–210.
79 Gkikas I, Palikaras K, Tavernarakis N. The role of mitophagy in innate immunity. *Front Immunol* 2018; 9: 1283.
80 Vermeulen K, Van Bockstaele DR, Berneman ZN. The cell cycle: a review of regulation, deregulation and therapeutic targets in cancer. *Cell Prolif* 2003; 36: 131–149.
81 Michaelis UR. Mechanisms of endothelial cell migration. *Cell Mol Life Sci* 2014; 71: 4131–4148.
82 O'Grady SM. CFTR involvement in cell migration and epithelial restitution. *In*: Progress in Understanding Cystic Fibrosis. London, IntechOpen, 2017.
83 Ng HP, Valentine VG, Wang G. CFTR targeting during activation of human neutrophils. *J Leukoc Biol* 2016; 100: 1413–1424.
84 Laval J, Anjali R, Dominik H. Neutrophils in cystic fibrosis. *Biol Chem* 2016; 397: 485.
85 Guggino WB. The cystic fibrosis transmembrane regulator forms macromolecular complexes with PDZ domain scaffold proteins. *Proc Am Thorac Soc* 2004; 1: 28–32.
86 Lim SH, Legere E-A, Snider J, *et al.* Recent progress in CFTR interactome mapping and its importance for cystic fibrosis. *Front Pharmacol* 2017; 8: 997.
87 Kunzelmann K, Mehta A. CFTR: a hub for kinases and crosstalk of cAMP and Ca2+. *FEBS J* 2013; 280: 4417–4429.
88 Pankow S, Bamberger C, Calzolari D, *et al.* ΔF508 CFTR interactome remodelling promotes rescue of cystic fibrosis. *Nature* 2015; 528: 510–516.
89 Castellani C, Quinzii C, Altieri S, *et al.* A pilot survey of cystic fibrosis clinical manifestations in CFTR mutation heterozygotes. *Genet Test* 2001; 5: 249–254.
90 Castellani C, Assael BM. Cystic fibrosis: a clinical view. *Cell Mol Life Sci* 2017; 74: 129–140.
91 Miller AC, Comellas AP, Hornick DB, *et al.* Cystic fibrosis carriers are at increased risk for a wide range of cystic fibrosis-related conditions. *Proc Natl Acad Sci USA* 2020; 117: 1621–1627.